

Structure and molecular properties of adsorbates at low coverage: Light-atom scattering from adsorbed Xe and CO

Hannes Jónsson and John H. Weare

*Department of Chemistry, University of California at San Diego,
La Jolla, California 92093*

Andrea C. Levi

*Università di Genova, Dipartimento di Fisica,
Via Dodecaneso 33, 16146 Genova, Italy*

(Received 7 May 1984)

A theory for light-atom scattering by low-coverage adsorbates on metal surfaces is presented. A model including attractive adatom potentials successfully explains data for CO and Xe adsorption. The radius of the repulsive potential for CO is found to increase by 10–20% upon adsorption. It is shown theoretically that random adsorption and island formation can be distinguished, all data for CO being consistent with the former. Xe data show both mechanisms, depending on coverage.

Recent experiments have shown light-atom scattering to be a very promising tool for studying surface adsorbates at low coverage.^{1–7} This technique is sensitive to very small amounts of adatoms on smooth metal substrates (coverage about 1%) and can, therefore, give unique information about isolated adatoms and their interaction. Poelsema, de Zwart, and Comsa¹ measured the specular scattering from CO adsorbed on very smooth Pt(111) and analyzed the limit of zero coverage in terms of a total cross section for the adsorbed CO. This cross section was somewhat larger than the gas-phase cross section (about 25%) but showed similar energy dependence. They concluded that the scattering by the adsorbate is dominated by the long-range attractive forces as is the gas-phase scattering. However, no theoretical support for this has been given. Light-atom scattering is very sensitive to surface defects. Poelsema, Verheij, and Comsa² measured the scattering from CO adsorbed on surfaces with defects and showed that light-atom scattering may provide a method for quantitative titration of defects as well as a method to study the migration of adsorbates on single-crystal surfaces. The scattering is also very sensitive to the arrangement of adatoms on the surface. Mason, Caudano, and Williams³ measured the incoherent elastic scattering as well as the specular intensity for CO and Xe adsorption on Cu(001) and found the coverage dependence in these two cases to be very different, showing different adsorption mechanisms. Poelsema, Verheij, and Comsa⁴ found a break in the specular versus coverage curve for Xe adsorption on Pt(111) at very low coverage (about 0.01) and ascribed this to a two-dimensional-gas–two-dimensional-solid phase transition which has not been seen using other techniques.

In previous theoretical work the light-atom scattering was formulated within the eikonal approximation and the surface and adsorbate represented by a hard wall with bumps corresponding to adatoms.^{7,8} The results provide interesting qualitative information but following the suggestion of Poelsema and co-workers that the long range attractive potential dominates the scattering, it is a question whether this model can be used to interpret data. Ibáñez and co-workers⁷ fitted this model to their data for CO on Ni(001) and found that the bumps on the hard wall had to be very large (one “CO-bump” covering 65 Å²).

In this Rapid Communication we present a theory for atom scattering from adsorbates at low coverage which includes long- and short-range adatom potentials. This model is found to give good agreement with both CO and Xe data. We find it essential to include the attractive part of the adatom potential. Using the gas-phase potentials for the adatoms we get excellent agreement for Xe and surprisingly good agreement for CO. Analyzing IR data⁹ we have determined that the effective electronic polarizability of CO adsorbed on Pt(111) is twice the polarizability of gas-phase CO. This implies that the attractive London force between the probe and CO is doubled. In order to agree with the scattering data, this increase in the attractive potential must be balanced by an increase in the repulsive potential. Very good agreement is obtained over the whole energy range both for He and H₂ scattering if the radius of the repulsive CO potential is increased by about 15%. This provides evidence for the predicted¹⁰ increase in electron density¹¹ at the CO upon adsorption.

It has often been argued from indirect evidence that CO molecules adsorbed on metal surfaces form islands (e.g., Ref. 9). We have found theoretically that light-atom scattering gives direct information on the arrangement of adatoms. Random adsorption leads to exponential decrease of the specular intensity with coverage while the growth of large islands is consistent with linear dependence. All the scattering data for CO adsorption^{1–7} shows exponential behavior and, therefore, no sign of island formation. The data for Xe, however, show linear dependence at higher coverage.^{3,4} At lower coverage there is a much steeper decrease which agrees very well with our calculations based on random adsorption. Our results, therefore, provide theoretical support for the interpretation of Poelsema *et al.*⁴ that a two-dimensional-gas–two-dimensional-solid phase transition was observed.

We consider the metal surface to be flat and characterized by perfect specular reflection, i.e., the surface potential only depends on the distance from the surface. In the asymptotic region the wave function has the form

$$\Psi_{\vec{k}}^{\pm} \sim e^{i\vec{k} \cdot \vec{r}} - e^{i(\vec{k}_s \cdot \vec{r} - \alpha)} + F(\Omega) \frac{e^{ikr}}{r}. \quad (1)$$

\vec{k} is the incoming wave vector and \vec{k}_s the specularly reflected wave vector. If I_0 is the incident intensity and A the cross-sectional area seen by the probe, the intensity falling into a solid angle $d\Omega$ in the direction of Ω' is

$$\frac{dI}{d\Omega}(\Omega') = I_0 \left[1 + \frac{4\pi}{kA} \text{Im}(e^{i\alpha} F) \right] \delta(\Omega' - \Omega_s) + \frac{|F|^2}{A} \quad (2)$$

where Ω_s is the solid angle in the specular direction. A relation similar to the optical theorem may be derived:

$$-\frac{4\pi}{k} \text{Im}[e^{i\alpha} F(\Omega_s)] = \int |F(\Omega)|^2 d\Omega \quad (3)$$

We introduce the t matrix t_m that completely describes the scattering by an isolated adatom at r_m and effective incoming wave $\Psi_{\vec{k}}^m$ that satisfies

$$\Psi_{\vec{k}}^m = \chi_{\vec{k}} + G_d^+ \sum_{n \neq m} t_n \Psi_{\vec{k}}^n \quad (4)$$

Here, χ is the wave function and $\langle r | G_d^+ | r' \rangle$ is the Green's function for scattering by the clean substrate. The scattering wave function is

$$\Psi_{\vec{k}}^{\pm} = \chi_{\vec{k}} + G_d^{\pm} \sum_m t_m \Psi_{\vec{k}}^m \quad (5)$$

If all the adatoms are identical and at the same distance from the surface, the scattering amplitude in the single scattering approximation ($\Psi_{\vec{k}}^m = \chi_{\vec{k}}$) is

$$F = \sum_m \exp[i(\vec{k} - \vec{k}') \cdot \vec{r}_m] f_A \quad (6)$$

f_A is the scattering amplitude for an isolated adatom placed above the origin and k' the outgoing wave vector.

f_A can be found by numerical means for arbitrary surface and adatom potentials. Here, we choose a model which is numerically simple while still giving good agreement with experimental data. The clean surface is taken to be a hard wall ($V_s = \infty$ when $z < 0$ and 0 when $z > 0$). Then $\alpha = 0$ and scattering by the adsorbate can be related to scattering by targets in the absence of a surface. The potential for these targets is the adsorbate's potential reflected in the surface plane. The scattering amplitude for an isolated adatom is

$$f_A(\vec{k} \rightarrow \vec{k}') = f(\vec{k} \rightarrow \vec{k}') - f(\vec{k} \rightarrow \vec{k}_s') \quad (7)$$

where $f(\vec{k} \rightarrow \vec{k}')$ is the scattering amplitude for scattering in the absence of a hard wall. Equation (7) results from the requirement that the wave function vanishes at the hard wall. The scattering from an adatom on a hard wall can, therefore, be reduced to a gas-phase scattering problem and well known numerical techniques (such as close coupling)

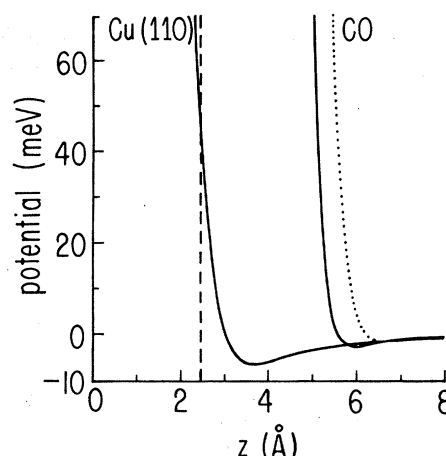


FIG. 1. Solid lines: the He-Cu(110) potential (Ref. 11) and the gas-phase He-CO potential (Ref. 12). Dotted line: the adjusted He-CO potential. The Cu surface atoms are centered at $z=0$ and the CO molecule is centered at the dashed line (Ref. 5).

can be used to find f_A for arbitrary adatom potentials.

We assume here that the adatoms are centered at the hard wall. This is a reasonable approximation as can be seen from Fig. 1, where a typical He-metal potential is shown¹¹ as well as the He-CO potential found by gas-phase scattering.^{5,12} The classical turning point of the He atom is nearly at the same distance from the surface as the center of the CO molecule. For hemispherical adatom potentials, $f(\vec{k} \rightarrow \vec{k}')$ can then be found using the familiar partial-wave method for central potentials. The true surface potential has an attractive well which we account for by refracting the incoming wave. For He we take the effective well depth to be $w = 2.3$ meV as determined by Poelsema, Palmer, de Zwart, and Comsa⁵ by comparing experimental curves for different angles. The results presented here are not very sensitive to this parameter. For H_2 we take w to be five times larger which is the ratio of the measured well depth of the H_2 -Ag(111) potential¹³ and a typical He-metal potential.

If the adatoms are randomly distributed on the surface, the specular intensity, to first order in the density n is [from Eqs. (2), (3), and (6)]

$$I_s = I_0 \left[1 - \frac{N\sigma_A}{A} \right] \quad (8)$$

where N is the number of adatoms seen by the probe

$$N = n \frac{A}{\cos\theta}$$

θ , is the refracted incoming angle and σ_A the total cross section for an isolated adatom. Second-order contributions come from both the single and double scattering:

$$\frac{dI'}{I_0 d\Omega} = -\frac{m^2}{2\pi^3 k A \hbar^4} \text{Im} \left[\lim_{\epsilon \rightarrow 0} \int \frac{d^3 k_2 \langle \chi_{\vec{k}_s} | t | \chi_{\vec{k}_2} \rangle \langle \chi_{\vec{k}_2} | t | \chi_{\vec{k}} \rangle}{k^2 - k_2^2 + i\epsilon} \beta_{\vec{k}}(\vec{k}_2) \right] \delta(\Omega' - \Omega_s) + \frac{|f_A|^2}{A} [N + \beta_{\vec{k}}(\vec{k}')] \quad (9)$$

where

$$\beta_{\vec{k}}(\vec{k}') \equiv \left\langle \sum_n \sum_{m \neq n} \exp[i(\vec{k} - \vec{k}') \cdot (\vec{r}_n - \vec{r}_m)] \right\rangle \quad (10)$$

For random adsorption on sites

$$\beta_{\bar{k}}(\bar{k}') = n^2 \frac{aA}{\cos\theta_r} \left[\frac{4\pi^2}{ak^2} \sum_G \frac{\delta(\Omega' - \Omega_{G+k_s})}{\cos\theta'} - 1 \right], \quad (11)$$

where G is the reciprocal lattice vector for the site lattice and a the area of the unit cell. Using the pole approximation to evaluate the first term in (9) leads to a cancellation of terms involving $\text{Re}[f_A(\Omega_s)]$. Terms with $G \neq 0$ can be neglected and the resulting contribution to the specular intensity is

$$\frac{I'_s}{I_0} = \frac{1}{2} \left(\frac{n\sigma_A}{\cos\theta_r} \right)^2 \left(1 + \frac{a \cos\theta_r}{2\sigma_a} \right). \quad (12)$$

The last term was estimated using Massey-Mohr approximation¹² and shown to be small. Combining this with (8) gives exponential behavior of the specular intensity at low density. If, however, the adsorbate forms large, perfect islands, we have found¹⁴ that β , and, therefore, I' is linear in n . Island formation is, therefore, consistent with a linear decrease of the specular intensity with coverage.

The low-coverage data for Xe⁴ adsorption on Pt(111) are in excellent agreement with our calculation assuming random adsorption and using the gas-phase He-Xe potential.¹⁵ The data give $\sigma_A = 94 \text{ \AA}^2$ while the calculated value is $\sigma_A = 97 \text{ \AA}^2$ ($v = 1740 \text{ m/s}$, $T_s = 80\text{--}90 \text{ K}$). Poelsema and co-workers^{1,4,5} reported $d(I/I_0)/dn$ in the limit of zero coverage and interpreted it as the adatom's total cross section. By our results this quantity is $\sigma_A/\cos\theta_r$, the cosine arising from the number of adatoms seen by the probe.

Figure 2 shows the measured energy dependence of the

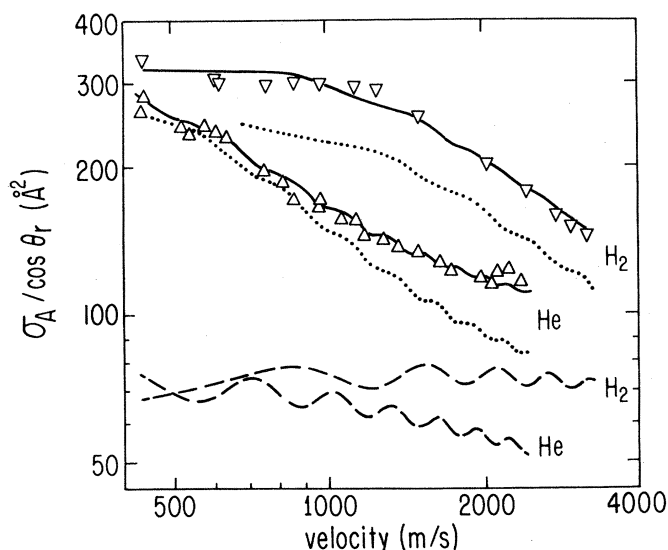


FIG. 2. H₂ and He scattering by CO adsorbed on Pt(111) (Ref. 1) at varying incident velocity and $\theta_i = 40^\circ$. ∇ is H₂ scattering; Δ is He scattering. Dotted lines: calculated He and H₂ scattering by CO using He-CO and D₂-CO potentials determined by gas-phase scattering ($R_m = 3.5 \text{ \AA}$, $\epsilon = 2.37 \text{ meV}$ and $R_m = 3.48 \text{ \AA}$, $\epsilon = 5.74 \text{ meV}$, respectively). Solid lines: calculated He and H₂ scattering using the adjusted potentials ($R_m = 4.3 \text{ \AA}$, $\epsilon = 1.38 \text{ meV}$ and $R_m = 4.04 \text{ \AA}$, $\epsilon = 4.69 \text{ meV}$, respectively). Dashed lines: calculated scattering from a hard hemisphere with radius equal to the classical turning point of the gas-phase D₂-CO or He-CO potentials.

He and H₂ scattering from CO on Pt(111).¹ Also shown is our calculation using LJ(12-6) potentials that were determined by fitting gas-phase scattering data.¹² The calculation is in qualitative agreement with the data. If, however, the attractive part of the CO potential is neglected and the adatom represented by a hard hemisphere, the calculated cross section (see Fig. 2) is much smaller and it does not have the right energy dependence. Figure 3 shows the He scattering data for CO on various substrates.^{3,5-7} The agreement with our calculation using the gas-phase potential is very satisfactory.

There is, nevertheless, a significant difference between the data and the calculation. This seems to be primarily due to a change in the CO potential upon adsorption. The refraction does not affect the He calculation very much and only at low energy; nor does changing the surface temperature between 90 and 300 K affect the measured He cross section over the whole energy range shown.^{5,16} This indicates that inelastic events do not substantially contribute to the adatom's total cross section. At rather high beam energy there is, furthermore, very good agreement with the Xe data. The measured angular dependence⁵ supports centering the molecule at the hard wall.¹⁴ The $\cos\theta_r$ factor accounts quantitatively for the increased apparent cross section with θ_i (except at glancing angles, $\theta_i > 70^\circ$, where the calculated cross section is too large). When the adatom is centered at the hard wall, σ_A is nearly independent of θ_i because the reflected adatom potential is spherically symmetric. The data, therefore, suggest a change in the CO potential.

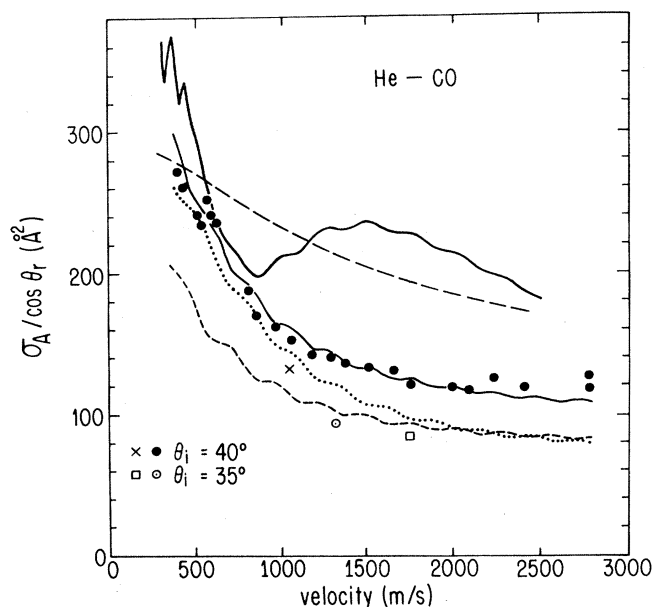


FIG. 3. He scattering by adsorbed CO at varying incident velocity. Data: \bullet are CO on Pt(111) (Ref. 5), \times are CO on Cu(001) transformed to $\theta_i = 40^\circ$ (Ref. 3), \circ are CO on Ni(110) (Ref. 6), and \square are CO on Ni(001) (Ref. 7). Dotted line and lower solid line: calculation using the gas-phase and the adjusted potential, respectively (also shown in Fig. 2). Upper solid line: calculation using doubled C_6 coefficient. --- Schiff-Landau-Lifshitz semiclassical approximation, which excludes glory oscillations, for potentials with doubled C_6 . ----- Calculation using gas-phase C_6 but increased C_{12} coefficient (classical turning point at 60 meV is moved out by 6%).

The scattering cross section is very sensitive to changes in the potential mostly due to the large glory oscillations (Fig. 3). It is not possible to predict how the cross section changes without doing quantum-mechanical calculations. When the C_6 coefficient of the potential is doubled in accordance with the increased electronic polarizability⁹ but the C_{12} coefficient left unchanged, the calculation looks qualitatively different from the data. (Orbiting resonances appear at low energy.) However, when C_6 is doubled and one parameter, the C_{12} coefficient, is adjusted to the data, very

good agreement is obtained over the whole energy range. (See Figs. 2 and 3. The adjusted He-CO potential is shown in Fig. 1.) The classical turning point of the adjusted He and H₂ potentials at 60 meV is moved out by 18% and 15%, respectively, as compared to the gas-phase potentials.

This work was supported in part by the National Science Foundation under Grant No. INT80-19908 and Consiglio Nazionale delle Ricerche CNRn 22.CT/81.00522.02/115.1827.

¹B. Poelsema, S. T. de Zwart, and G. Comsa, Phys. Rev. Lett. **49**, 578 (1982); **51**, 522 (1983).

²B. Poelsema, L. K. Verheij, and G. Comsa, Phys. Rev. Lett. **49**, 1731 (1982).

³B. F. Mason, R. Caudano, and B. R. Williams, Phys. Rev. Lett. **47**, 1141 (1981).

⁴B. Poelsema, L. K. Verheij, and G. Comsa, Phys. Rev. Lett. **51**, 2410 (1983).

⁵B. Poelsema, R. L. Palmer, S. T. de Zwart, and G. Comsa, Surf. Sci. **126**, 641 (1983).

⁶H. Wilsch and K. H. Rieder, J. Chem. Phys. **78**, 7491 (1983).

⁷J. Ibáñez, N. García, and J. M. Rojo, Phys. Rev. B **28**, 3164 (1983); J. Ibáñez, N. García, J. M. Rojo, and N. Cabrera, Surf. Sci. **117**, 23 (1982).

⁸A. C. Levi, R. Spadacini, and G. E. Tommei, Surf. Sci. **108**, 181 (1981); **121**, 504 (1982).

⁹See, H. Ibach and D. L. Mills, *Electron Energy Loss Spectroscopy and*

Surface Vibrations (Academic, New York, 1982), Chap. 3.4.4. Using the data of H. J. Krebs and H. Lüth [Appl. Phys. **14**, 337 (1977)] we calculate $\alpha_e = 4.9 \text{ \AA}^3$ as compared to the gas phase $\alpha_e = 2.5 \text{ \AA}^3$.

¹⁰D. W. Bullett and M. L. Cohen, Solid State Commun. **21**, 157 (1977).

¹¹J. Harris and A. Liebsch, Phys. Rev. Lett. **49**, 341 (1982).

¹²H. P. Butz, R. Feltgen, H. Pauly, and H. Vehmeyer, Z. Phys. **247**, 70 (1971).

¹³C. F. Yu, K. B. Whaley, C. S. Hogg, and S. J. Sibener, Phys. Rev. Lett. **51**, 2210 (1983).

¹⁴H. Jónsson, J. H. Weare, and A. C. Levi, Surf. Sci. (to be published).

¹⁵K. M. Smith, A. M. Rulis, G. Scoles, R. A. Aziz, and V. Nain, J. Chem. Phys. **67**, 152 (1977).

¹⁶B. Poelsema, L. K. Verheij, and G. Comsa, Surf. Sci. (to be published).